A Truly In-shoe Force Measurement System

by

Abhishek Badarinath

A Thesis Presented in Partial Fulfillment
of the Requirements for the Degree
Master of Science

Approved January 2018 by the
Graduate Supervisory Committee:

Sayfe Kiaei, Chair
Bertan Bakkaloglu
Jennifer Kitchen

ARIZONA STATE UNIVERSITY

May 2018

ABSTRACT

In this work, the development of a novel and a truly in-shoe force measurement system is reported. The device consists of a shoe insole with six thin film piezo resistive sensors and a main circuit board. The piezo resistive sensors are used for the measurement of plantar pressure during daily human activities. The motion sensor mounted on the main circuit board captures kinematic data. In addition, the main circuit board is responsible for the wireless transmission of the data from all the sensors in real-time using BLE protocol. It is housed within the midsole of the shoe, under the medial arch of the foot. The real-time quantitative data and its analyses, enables athletic performance evaluation, biomedical ailment detection and everyday fitness tracking. A test subject walked 20 steps on a flat surface at a comfortable speed wearing a shoe fitted with the insole and the main circuit board. Measurements were captured using a BLE enabled laptop and the test results were validated for accuracy. From the real-time data captured, the number of steps walked, the speed and the plantar pressure applied can be clearly established. Moreover, additional kinematic data from the motion sensor was captured. Further processing of kinematic data using techniques such as machine learning is essential to get meaningful inferences.

ACKNOWLEDGMENTS

I would like to express my gratitude to my advisor Dr. Sayfe Kiaei for giving me the opportunity to work on this project. His advice and support played a crucial role in the completion of this work. I am grateful to Dr. Bertan Bakkaloglu, Dr. Jennifer Kitchen, and Dr. James Abbas for their time and support as members of my thesis committee. I am also grateful to Mr. Timothy Markison for his support and motivation throughout the course of this project.

Secondly, I would like to thank Dr. Jaehyun Park for his invaluable support during the initial phase and Shreerang Dabade for helping me with testing and post-processing during the final stages of this work. Finally, thanks to Ashwath Hegde for his support on various topics through technical discussion.

TABLE OF CONTENTS

Page

LIST OF TABLES v

LIST OF FIGURES vi

CHAPTER

1. INTRODUCTION 1

    1.1 Motivation 1

    1.2 Applications 2

    1.3 Literature Survey 3

    1.4 Proposed System 5

2. SYSTEM ARCHITECTURE 6

    2.1 Overview of System Architecture 6

    2.2 Pressure Sensor Selection 7

    2.3 Design and Fabrication of Insole 9

3. CIRCUIT BOARD DESIGN 11

    3.1 Component Selection 11

        3.1.1 MCU CC2650 11

        3.1.2 MPU 9250 12

        3.1.3 Operational Amplifier 13

    3.2 Analog Front End Design 13

CHAPTER Page

3.3 CC2650 Reference Design 14

3.4 MPU9250 Reference Design 16

3.5 Design and Fabrication of Circuit Board 16

4. SOFTWARE DEVELOPMENT 19

4.1 Overview of Software Components 19

4.2 Sensor Controller Driver Development 20

4.3 Application Software Development 21

4.3.1 ADC 21

4.3.2 MOV 21

4.4 Custom Bluetooth Profile Development 22

5. RESULTS 23

5.1 Experimental Procedure 23

5.2 Results from the Smart Shoe 23

6. CONCLUSION 31

REFERENCES 33

LIST OF TABLES

Table Page

1. Location of Pressure Sensor under the Foot 9

2. Digital IOs and Their Function 15

3. Antenna Specifications 17

4. Main Circuit Board Dimensions 18

5. Software Modules and Their Function 21

6. Summary of All the Parameters from Post-processing 24

LIST OF FIGURES

Figure Page

1. Adidas Micoach and Nike + iPod Devices 3

2. Novel's Pedar and Tekscan's F-Scan System 4

3. System Architecture of the Force Measurement System 6

4. FSR Sensor Used for Force Measurement 7

5. Resistance vs Weight of FSR 8

6. Conductance vs Weight of FSR 9

7. Fabricated Insoles with FSR's Location 10

8. Block Diagram of the CC2650 MCU 11

9. Interface from FSR sensor to MCU 13

10. CC2650 Reference Design Schematic 14

11. MPU9250 Reference Design Schematic 16

12. Block Diagram of the Main Circuit Board 16

13. Inverted F Antenna Layout 17

14. Layout of the Main Circuit Board (Front and Back) 18

15. Fabricated Main Circuit Board (Front and Back) 18

16. Software Architecture 19

17. ADC and Its Input Arrangement 20

18. ADC Sampling BLE Service 22

19. Algorithm Used for the Post-processing Script 24

20. Filtered Data from FSR1 25

21. Filtered Data from FSR2 25

Figure Page

22. Filtered Data from FSR3 26

23. Filtered Data from FSR4 26

24. Filtered Data from FSR5 27

25. Filtered Data from FSR6 27

26. Filtered Data from All the FSR Sensors 28

27. Filtered Data from the Accelerometer X Axis 29

28. Filtered Data from the Accelerometer Y Axis 29

29. Filtered Data from the Accelerometer Z Axis 30

30. Smartphone App Interface 31

CHAPTER 1

1 INTRODUCTION

1.1 Motivation

Performing an athletic movement requires a high level of accuracy for proper kinematic execution. However, they are often difficult to quantitatively measure. Thus, many athletes depend on ‘look and feel’ in performing an athletic movement [21]. Acquiring data of the precise kinematics involved in an athletic movement could be useful for a reliable and accurate measurement of the dynamics involved.

Currently, the methods available to analyse these movements require heavy equipment, like high speed video cameras. An advanced setup is required for such analyses, which is impractical to be taken on the field. Other methods include coaches monitoring the athlete’s movements and athletes themselves doing the analyses. Drawback with such methods is that the conclusions will be based on ‘look and feel’ [21], which can be different from the actual biomechanics happening during the movements.

This work provides a method, without requiring heavy equipment, for capturing the pressure and kinematic data in real-time from the feet. As explained by Abhay et al. [21], this may not fully account for the movements being performed in the other parts of the body but will be useful to understand the footwork, which forms the foundation of the rest of the motion. The real-time quantitative data and its analyses, through this work, will enable coaches and athletes to better understand the performance specifications, detect minute errors and make the corrections required to achieve the ideal motion.

1.2 Applications

As described by Abhay et al. [21], athletic motions are high precision kinematic movements to generate the right amount of power and accuracy in any sport. These results are difficult to achieve without a solid foundation, which are the stance and the footwork. As these kinematic motions involve high speeds and intense forces on different muscles, slight deviations from ideal movements can lead to injuries. Therefore, understanding the kinematics and performing motions according to it is highly desirable. As described in motivation, the analyses of the quantitative data provide a way to improve athletic performance and to prevent related injuries.

Gait analysis helps in understanding the biomedical abnormalities that occur in the human body while performing everyday kinematic motions like walking. Lack of knowledge of proper gait can lead to application of unnecessary forces on the feet leading to imbalances, improper form, and even injuries. As our feet are the weight bearers of our body while performing most of the kinematic motions, problems with the feet not only affect them but also the joints above them [21]. This work makes the gait analysis faster and a more portable process. Access to the quantitative data makes it possible for anyone to measure the forces they are applying on their feet while performing different daily activities. This allows them to correct minute errors in their foot positioning and basic walking form.

Over the past few decades, footwear's have seen numerous advancements with respect to the comfort, fit, and material. However, no breakthrough products have been developed that change the way we perceive footwear presently. It is trailing far behind other products

such as smart watches, fitness bands etc. that are smarter and provide seamless digital experience. This work presents one such idea of a smart shoe that can be used for everyday activity tracking. From the quantitative data available, it is possible to evaluate step count, distance travelled, calories burnt and many more fitness parameters.

1.3 Literature Survey

There have been several attempts at making a shoe smarter especially for fitness tracking. Nike had developed a capsule like device back in the days when iPod was popular. The product was a personal workout assistant called Nike + iPod. The focus was to track workouts. However, the device did not have any additional capabilities such as fitness tracking that we would expect from a smart shoe. Similarly, Adidas had its own version called the micoach. Even this was mainly designed for tracking workouts and capturing METs. Both, illustrated in Figure 1, lacked additional capability of what a smart shoe can do with pressure sensors.

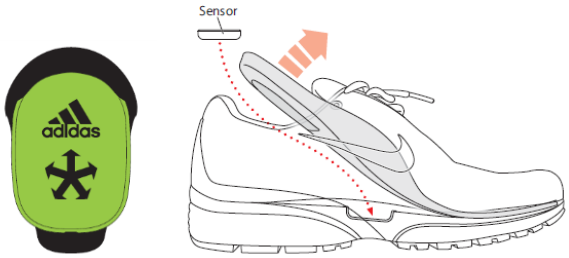

Figure 1: Adidas Micoach and Nike + iPod Devices

There are several pressure mapping systems that use pressure sensors, solely developed for biomedical applications. For instance, Tekscan's F-Scan system and Novel's Pedar system, which are used for data acquisition, are currently used for determining biomedical

ailment through Pedobarography. As illustrated by Hurkmans et al. [6], Hessert et al. [10], Han et al. [17], and Brown et al. [18], these devices are designed for high resolution measurements under specific settings. In addition, Saito et al. [5] highlighted the dynamic applications in which these devices were used and noted several limitations. Firstly, they are not truly insole devices and require a special recording equipment to be worn. Secondly, the data acquisition is not real time and the analysis of the data is done after the recording device is connected to a PC. Finally, they are simply not designed for everyday usage. If there was a way to eliminate the above drawbacks, the resulting device could be used for tracking athletic performance as well. Currently, there are no footwear products that meet these requirements.

Figure 2: Novel's Pedar and Tekscan's F-Scan system

Apart from the commercial attempts at smart shoe, there are several prior arts that come close to fulfilling the motivation of this work. Hui et al. [1] presented a shoe system for plantar pressure measurement and gait phase detection. The shoe uses reliable strain gauges for plantar pressure evaluation. However, the major drawback of the design is the signal processing board, which must be worn on the ankle of the foot. Moreover, the measurement system presented is not designed to be truly insole. Kyoungchul Kong and Tomizuka [2] presented a similar system for gait monitoring using air pressure sensors embedded within the shoe. They have the same drawback of requiring several components of the system to

be placed at the back of the shoe. Stacy et al. [4] developed an insole with sixteen sensors that was designed for data acquisition. The focus was to assess balance by detecting subtle changes in the weight distribution. However, the device is not truly insole and possess serious limitations with respect to the comfort and usage. When the device is worn, the cables run along the sides of the shoe and must be physically connected to the receiver. Thus, it is not practical for everyday usage.

1.4 Proposed System

The goal of this work is to develop a truly in-shoe solution for measuring plantar pressure and kinematic data from the foot. The system should work without the need of any recording devices to be worn, which ensures that it is suitable for everyday use and for sports application. Moreover, all the components of the system should be located entirely within the shoe (no visible parts like cables etc.). It should also transmit the measured data in real-time over Bluetooth Low Energy (BLE) protocol, which can be received by a BLE enabled smartphone or laptop.

CHAPTER 2

2 SYSTEM ARCHITECTURE

2.1 Overview of System Architecture

The simplified architecture of the system is illustrated in the Figure 3.

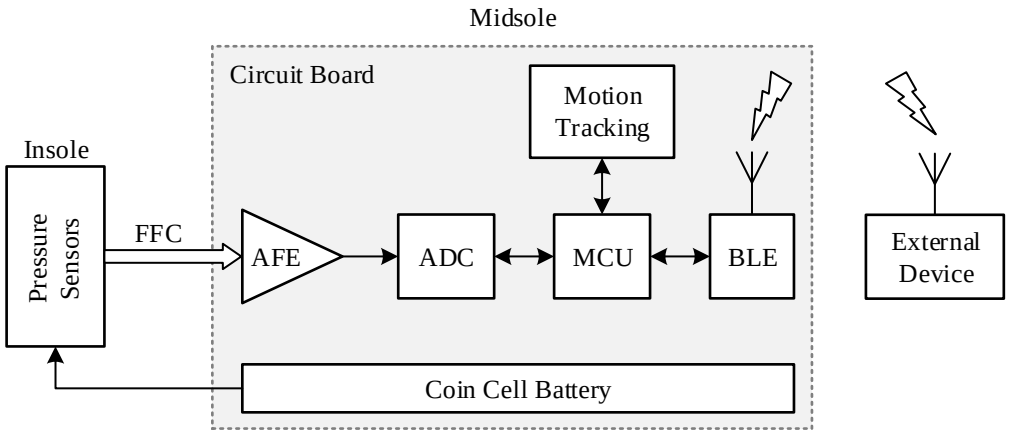

Figure 3: System Architecture of the Force Measurement System

The system itself consists of two parts that work together. First, it consists of a flexible insole with pressure sensors, placed inside the shoe (under the insole of the shoe). Second, the main circuit board with all the processing components and the motion tracking sensor, which rests in the hard midsole section of the shoe. All the sensors and processing components are powered with a coin cell battery. The insole and the main circuit board are connected using a Flat Flexible Cable (FFC). The pressure sensors from the insole are connected to the amplifier, which presents the variation in pressure as voltage to the ADC, which is connected to the MCU. The data is then sampled by the MCU and transmitted over BLE. In addition, the kinematic data from the motion tracking sensor is captured by

the MCU and transmitted over BLE. The real-time data can be captured using a BLE capable external device (mobile or laptop).

2.2 Pressure Sensor Selection

As discussed by Hurkmans et al. [6], there are different ways of measuring weight bearing. For this work, the focus is on linearity, reliability, and form factor. Thus, thin film resistive sensors are used, which are great for an insole due to its low profile. Moreover, they are easy to integrate and achieve reasonable accuracy. Figure 4 shows the thin film piezo resistive force sensor used for measuring plantar pressure. The smallest version of the sensor has the following external dimensions 25.4mm × 14.0mm × 0.20mm. In addition, the diameter of the sensing area is around 9.53mm. These sensors can measure weight bearing of up to 100lb each.

Figure 4: FSR Sensor Used for Force Measurement

Changing electrical resistance is the main principle with which the weight bearing is estimated. When no weight is applied, the sensor would offer infinite resistance. As weight is applied, the electrical resistance reduces. Figure 5 shows the relation between weight applied and resistance offered by the sensor. The values were obtained by measuring the resistance offered by the sensor when weight was applied using a hydraulic press. Readings were taken with insole only and by placing the insole within the shoe and applying pressure

over the sole of the shoe. The amount of pressure detected by the sensor when placed under the sole of the shoe is reduced. Thus, it is important to calibrate the sensors to precisely adjust the range and the resolution of the measurement. This is achieved with the help of the interface circuitry presented in the next section.

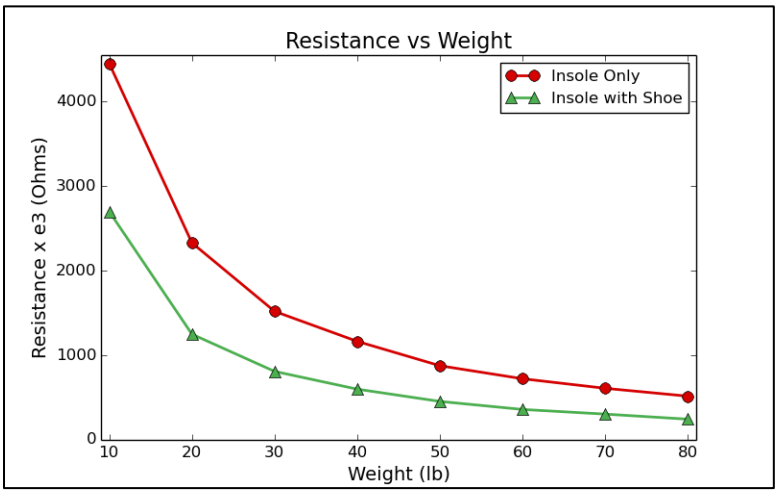

Figure 5: Resistance vs Weight of FSR

The conductance of the sensor provides us with the information about the linearity of the measurement. For the insole with shoe case, the conductance vs weight is plotted in Figure 6. The near straight line is an indication of the linearity of the measurements obtained.

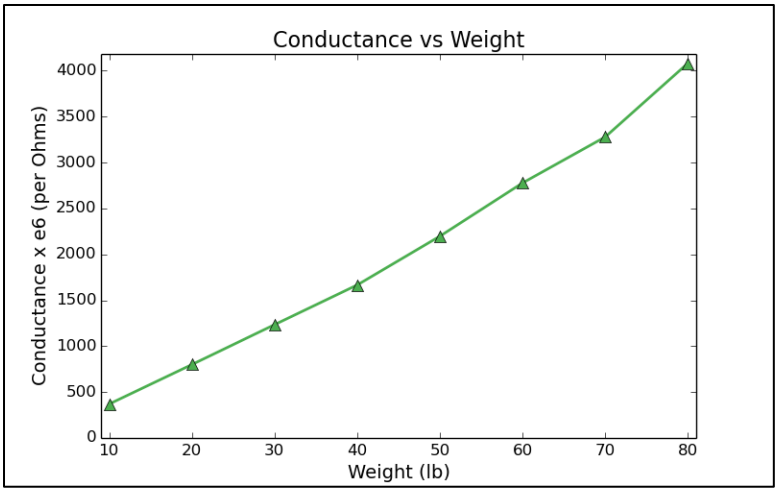

Figure 6: Conductance vs Weight of FSR

2.3 Design and Fabrication of Insole

To accurately measure the plantar pressure distribution during various activities, it is essential to have the sensors located at the precise locations under the foot. From the foot pressure distribution analysis done by Hessert et al. [10], the points at which maximum pressure distribution is expected is known. Six thin film sensors are used to cover the major points where plantar pressure distribution is maximum. Two sensors covering the heel of the foot (medial and lateral calcaneus), two sensors at the metatarsal, and two sensors at the top (hallux and toe) respectively. Table 1 summarizes the location of each sensor.

Table 1: Location of Pressure Sensor Under the Foot

Sensor	**Location**
FSR1	Toe
FSR2	Hallux
FSR3	Metatarsal
FSR4	Metatarsal
FSR5	Lateral calcaneus
FSR6	Medial calcaneus

The insole itself is made from flexible PCB so that it can be comfortably placed between the midsole and the actual insole of the shoe. Figure 7 shows the insoles that were fabricated. The white circles indicate the locations under the foot where the pressure sensors are mounted (refer Table 1).

Figure 7: Fabricated insoles with FSR's location

CHAPTER 3

3 CIRCUIT BOARD DESIGN

3.1 Component Selection

3.1.1 MCU CC2650

TI's MCU CC2650 was chosen for this design. The block diagram of the MCU is shown in the Figure 8.

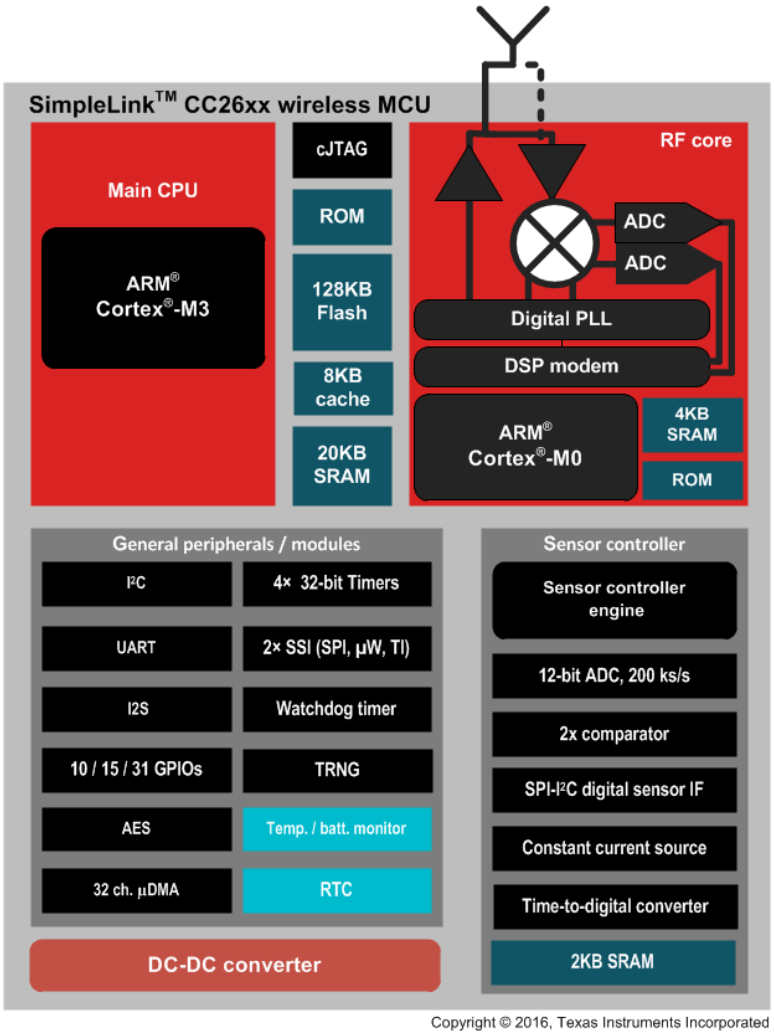

Figure 8: Block Diagram of the CC2650 MCU

The choice was based on the match between the system architecture and the peripherals available within the MCU. For instance, the MCU's Sensor Controller is equipped with a 12-bit ADC capable of 200k samples/sec along with an 8-channel MUX. This could be used to sample plantar pressure data from up to eight external pressure sensors. The RF core could be used to send and receive information wirelessly using BLE protocol. The I^2C peripheral could be used to communicate with the motion sensor that is on the main circuit board. The UART peripheral could be used during development for debugging purposes. In addition, TI's embedded software platform (Code Composer Studio) is extremely powerful and well documented, which helps during the development of the software for the MCU.

3.1.2 MPU 9250

To track motion, the MPU 9250 from InvenSense was chosen. It is a 9-axis motion tracking device that combines 3-axis gyroscope, 3-axis accelerometer and 3-axis magnetometer. The MPU has three 16-bit ADCs that digitize the measurements done by the 9-axis motion sensor. The digitized output is then transmitted using I^2C to the MCU. In addition, the full-scale range of accelerometer and gyroscope are user-programmable, which provides flexibility to set the sensitivity of measurement. Moreover, it supports features such as wake on detection. This could help in saving power when motion is not detected for a predefined time.

3.1.3 Operational Amplifier

Analog front end is needed to measure the changes in plantar pressure as variation in either voltage or current. This information is then digitized with the help of an ADC found within the MCU. For this purpose, a precision operational amplifier LPV811 is used. It consumes extremely less quiescent current of 450nA, which was a major consideration in choosing the device. Other features include rail-to-rail swing at the output, which translates to wide range of plantar pressure measurement.

3.2 Analog Front End Design

To translate the variations in plantar pressure into a measurable voltage, the interface circuit shown in the Figure 9 is used. As illustrated, one end of the FSR, from the insole, is connected to the reference voltage V_{REF} and the other end to the amplifier's noninverting input terminal. In addition, a feedback resistor R_F is connected between the inverting terminal and the output of the amplifier. This arrangement allows us to measure the variation in pressure as voltage V_{FSR} at the output terminal of the amplifier. The relation between resistance of the FSR and output V_{FSR} of the amplifier is given below.

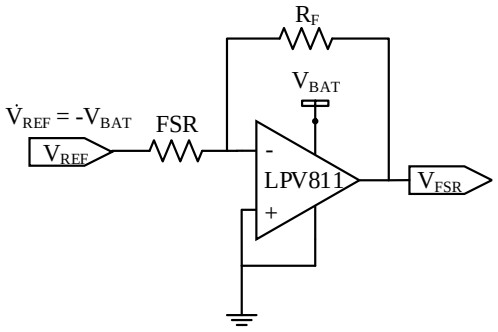

Figure 9: Interface from FSR Sensor to MCU

$$V_{FSR} = -V_{REF} * \frac{R_F}{FSR}$$

When no pressure is applied, the output voltage of the amplifier is zero since the FSR has infinite impedance. When pressure is applied, FSR's impedance decreases and the voltage gradually rises and is proportion to the amount of pressure applied. The maximum value of the output is close to V_{BAT}. Beyond this point, the output voltage will not change with increase in pressure. Furthermore, by adjusting R_F, the range and resolution of output voltage can be controlled. This is essential for the calibration of the sensor. To start with, the value of R_F is chosen as 200kΩ and VREF as -3V. Since V_{FSR} saturates at 3V, we can determine the pressure variation of up to 70 – 80lb per sensor (equivalent of FSR's resistance reaching 200kΩ).

3.3 CC2650 Reference Design

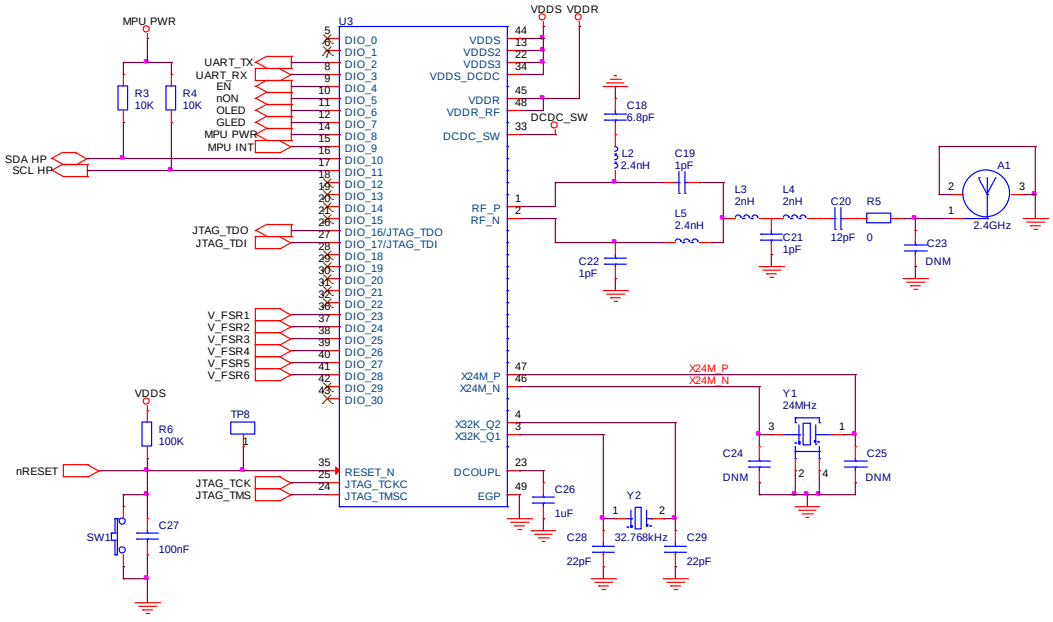

Figure 10: CC2650 Reference Design Schematic

Figure 10 shows the reference design used for the MCU CC2650. From the device's datasheet, the differential RF front-end configuration option is used, which ensures best performance. In addition, the choice of the crystal oscillators and the coupling capacitors (for supply and ground) are based on the reference designs from TI. For this work, to measure plantar pressure, six FSRs are connected to the analog pins of the MCU. These pins are from the 8-channel MUX that is internally connected to the MCU's ADC. All the other digital IOs used and their function are listed in the Table 2.

Table 2: Digital IOs and their Function

Pin	**Name**	**Function**
DIO_2	UART_TX	For TX and RX of debugging information during development over UART.
DIO_3	UART_RX	
DIO_4	EN	Enable/disable power to amplifiers
DIO_5	nON	Enable/disable power to inverter
DIO_6	OLED	Orange LED for system status notification
DIO_7	GLED	Green LED for BLE status notification
DIO_8	MPU PWR	Enable/disable power to MPU 9250
DIO_9	MPU INT	Interrupt signal from MPU 9250
DIO_10	SDA	Serial Data Line from MPU 9250
DIO_11	SCL	Serial Clock Line from MPU 9250
DIO_23 to DIO_28	V_FSR1 to 6	Interface circuit output voltages

For convenience during development, a reset switch is included, which directly restarts the MCU. The JTAG connection is included to enable flashing and debugging of the MCU's software.

3.4 MPU9250 Reference Design

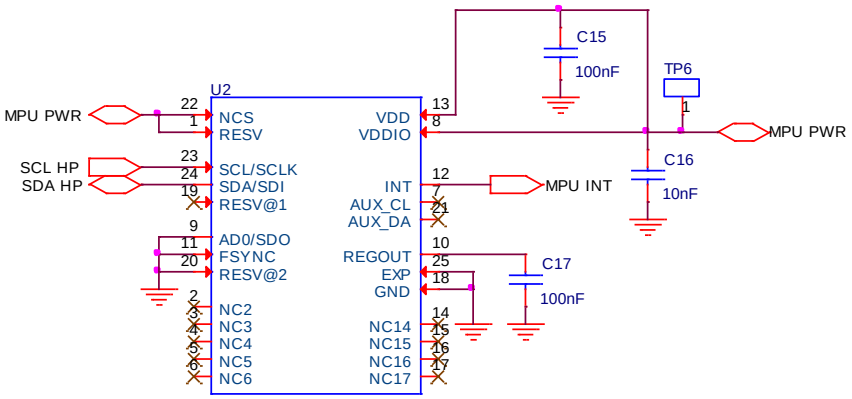

Figure 11: MPU9250 Reference Design Schematic

Figure 11 shows the reference design used for MPU 9250. The MPU is powered from a digital pin (MPU PWR) of the MCU. Thus, the MCU's software can control whether to enable or disable MPU's power at any time. The MPU INT pin generates interrupt to indicate that the data is available for MCU to be read. It is also used to indicate that the motion was detected (wake on motion interrupt). The data is exchanged between the MPU and MCU using I^2C protocol using Serial Data Line (SDA) and Serial Clock Line (SCL).

3.5 Design and Fabrication of Circuit Board

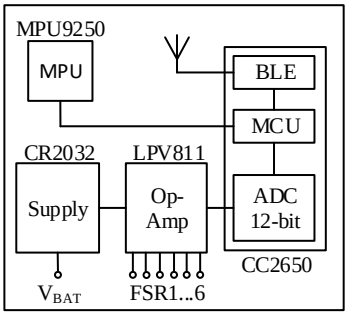

Figure 12: Block Diagram of the Main Circuit Board

The block diagram of the main circuit board is presented in Figure 12. It has all the components that are necessary for processing and transmission of data in real-time. The board is powered with the help of a coin cell battery – CR2032. The focus during the design was to reduce the footprint as much as possible. This is essential to ensure that the resulting circuit board fits comfortably within the midsole section of the shoe. The components that require a lot of area are the CC2650 reference design (described above), the coin cell battery holder and the antenna.

A 2.4GHz inverted F antenna recommended by Texas Instruments was used in this design. The specifications of the antenna used are listed in the Table 3.

Table 3: Antenna Specifications

Parameter	**Value**
Gain (XZ plane)	+3.3 dBi
Bandwidth	2.3 – 2.7 GHz
Length	25.7 mm
Height	7.5 mm

From the specifications, the antenna is compact and provides good performance. The actual layout of the antenna is illustrated in the Figure 13.

Figure 13: Inverted F Antenna Layout

The PCB layout with all the components are illustrated in the Figure 14. The components highlighted in Yellow (reset SW, UART connector and external supply connector) are used during development of software for debugging purposes. These can be

removed once the board works as expected. In addition, a lot of area can be saved once these components are excluded from the layout for the subsequent versions of the PCB.

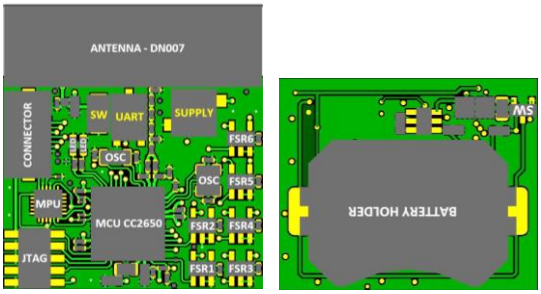

Figure 14: Layout of the Main Circuit Board (Front and Back)

The board dimensions are highlighted in the Table 4. The dimensions ensure that it can be easily accommodated within the midsole of a typical sports shoe.

Table 4: Main Circuit Board Dimensions

Parameter	**Dimension**
Width	2.75 cm
Length	3.00 cm
Height	0.70 cm
Layers	4
Area	8.25 cm^2

Figure 15 is the picture (front and back) of the actual PCB that was printed as the first prototype. This was used for the development and verification of the software.

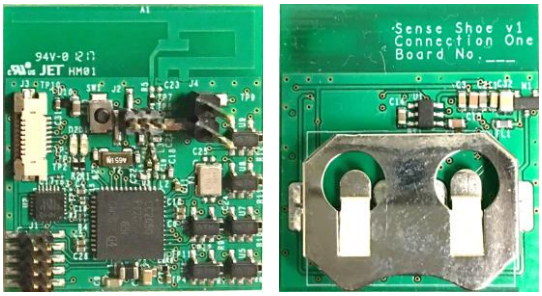

Figure 15: Fabricated Main Circuit Board (Front and Back)

CHAPTER 4

4 SOFTWARE DEVELOPMENT

4.1 Overview of Software Components

The MCU CC2650 used for this work is from TI. Thus, TI's environment (Code Composer Studio), RTOS and BLE stack are used for the development of the software. The RTOS and BLE stack components used are specifically designed for the CC26XX MCU family. Figure 16 shows the development system with all the software components.

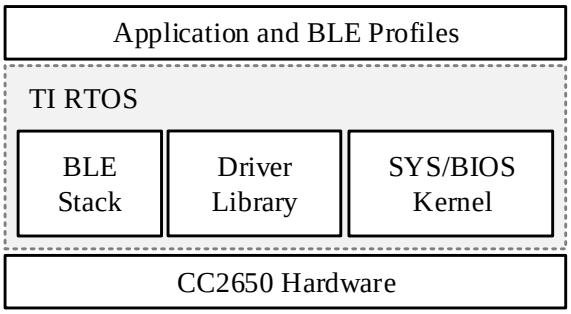

Figure 16: Software Architecture

BLE stack component provides the necessary libraries to implement the BLE services. These services form the basis to send and receive information over BLE. BLE profiles are developed in application layer to tailor the BLE messages based on the application's requirement. Driver Library is the abstraction layer between the CC2650 registers and the software. This layer provides a way to control the CC2650 hardware. The SYS/BIOS Kernel provides peripheral drivers for components such as I^2C, UART etc. and power management support. In addition, it supports thread types for variety of situations. These include hardware interrupts, software interrupts, tasks, idle functions and, periodic

functions. It is responsible for real-time scheduling and synchronization. Thread synchronization includes semaphores, events, gates and mailboxes.

4.2 Sensor Controller Driver Development

From the system architecture in Figure 3, the ADC is one of the key hardware components for this system. It is crucial because it must continuously sample data from all the six pressure sensors connected to its input. The arrangement is illustrated in the Figure 17.

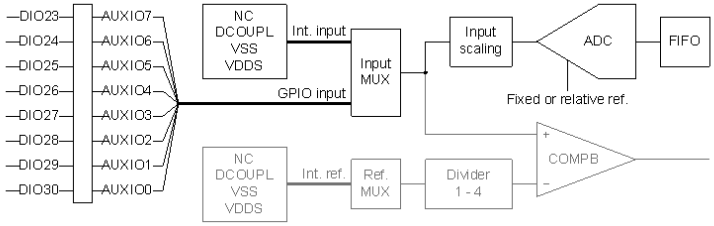

Figure 17: ADC and Its Input Arrangement

Thus, saving power at the driver level ensures that the power consumption for the overall system reduces. For this purpose, a custom driver was developed to control the function of the ADC based on the applications requirement. The application software issues an execute command to the driver. The command from the application includes ADC channel that needs to be sampled. Once the command is issued, the application waits for the driver to sample data from the corresponding ADC channel and fill the buffer. After the measurement is complete, the driver generates a hardware interrupt to notify the application that the data is available in the buffer. The application receives and clears the

interrupt and reads the ADC channel data from the buffer and starts additional processing of the data.

4.3 Application Software Development

The application software consists of modules that interact with the RTOS and BLE stack services to implement the required functionality. There are four modules, each implemented as a system task, that perform a specific function. The modules and their operations are listed in the Table 5.

Table 5: Software Modules and their Function

Module	**Function**
ADC	Handles communication with Sensor Controller (ADC)
MOV	Handles communication with MPU9250
BAT	Responsible for battery management
LED	Responsible for indicating system status

4.3.1 ADC

The ADC module has a single task that is executed periodically. The task requests the Sensor Controller driver to perform sampling of a specific ADC channel to which a FSR sensor is connected. Once the measurement is done, an interrupt is generated by the Sensor Controller. Upon receiving the interrupt, the ADC task resumes and retries the data from the buffer and sends it over BLE.

4.3.2 MOV

The MOV module is responsible for gathering movement data from the motion processor MPU9250. The module communicates with MPU9250 periodically using I2C

protocol. The individual components of the processor such as accelerometer, gyroscope and the magnetometer can be either enabled or disabled. By default, all the components are enabled and the data received from MPU9250 is transmitted over BLE.

4.4 Custom Bluetooth Profile Development

Each module that wants to send information over BLE needs to have a BLE service to interact with the BLE stack. For this purpose, the Bluetooth Developer Studio (BDS) was used to develop services for each module. In total, there are three BLE services for ADC, MOV and BAT modules respectively. Each BLE service contains entries such as name of the service, the identifier (UUID), number of bits for the identifier, the type of operation the BLE service can perform (read, write, notify etc.), and the data fields. Figure 18 is an example of ADC sampling BLE service developed using the BDS.

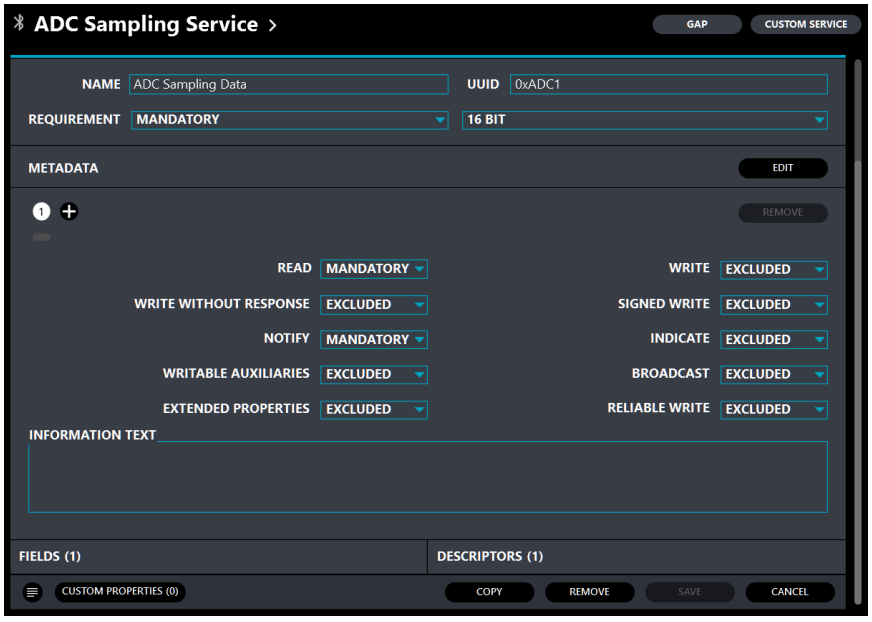

Figure 18: ADC Sampling BLE Service

CHAPTER 5

5 RESULTS

5.1 Experimental Procedure

A slot large enough to accommodate the main circuit board was cut open in the midsole (under the medial arch of the right foot) of a sports shoe. The board was secured in the slot so that the motion data captured is accurate and free of distortions. The insole was placed over the midsole and the board was connected. The arrangement is now capable of measuring and transmitting pressure and motion data over BLE.

One healthy subject (male, 26 years) with body weight of 185lb. wore the shoe and walked 20 steps on a flat surface at a comfortable speed. While he was walking, the data packets transmitted over BLE were being captured with a laptop running BLE monitor application. Data from several attempts were captured and saved on the laptop for post processing. Between attempts, the speed of walking and number of steps walked were altered. The data captured from these experiments were processed using Python script.

5.2 Results from the Smart Shoe

Figure 20 through Figure 25 represent the filtered data captured from all the pressure sensors placed on the insole under the right foot. The filtered data is the outcome of passing the original data through a 5-point moving average filter to reduce high frequency noise. From the data, we can make several quick observations. First, the number of peaks represent one half of the number of steps walked, which is 10 (or 20 steps) in this case. Second, the height of the peak indicates the amount of force applied during walking. Higher

peaks indicate larger force applied during walking from the corresponding regions of the right foot. For instance, the peaks are highest from FSR2, which indicates that the force from the hallux region of the right foot is the largest. Third, the distance between the peaks can be used to extract the walking speed. Since we know the typical stride length (distance per step) and the sampling frequency (time), the walking speed can be calculated. Figure 19 illustrates the algorithm used in the script to determine the above parameters. Table 6 summarizes the information that could be extracted from the filtered data. The average values of all the parameters were evaluate over the time interval of 20s.

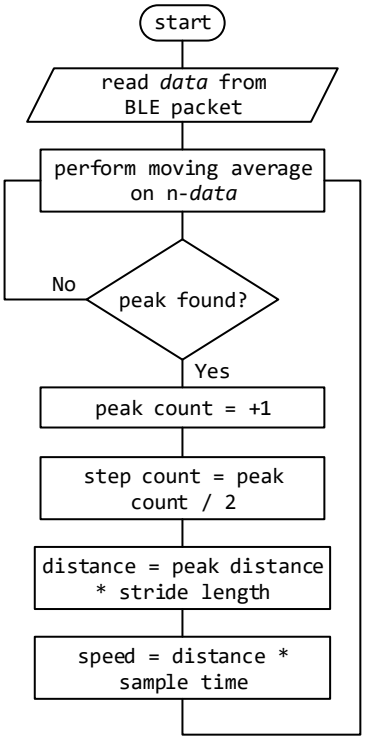

Figure 19: Algorithm Used for the Post-processing Script

Table 6: Summary of All the Parameters from Post-processing

Parameter	**Result**
Peaks detected	10
Average steps	20

Sampling frequency	10Hz
Average distance	12.8m
Average speed	0.64m/s
Average force from FSR1	657.64N
Average force from FSR2	1434.68N
Average force from FSR3	1064.38N
Average force from FSR4	742.24N
Average force from FSR5	332.54N
Average force from FSR6	275.77N

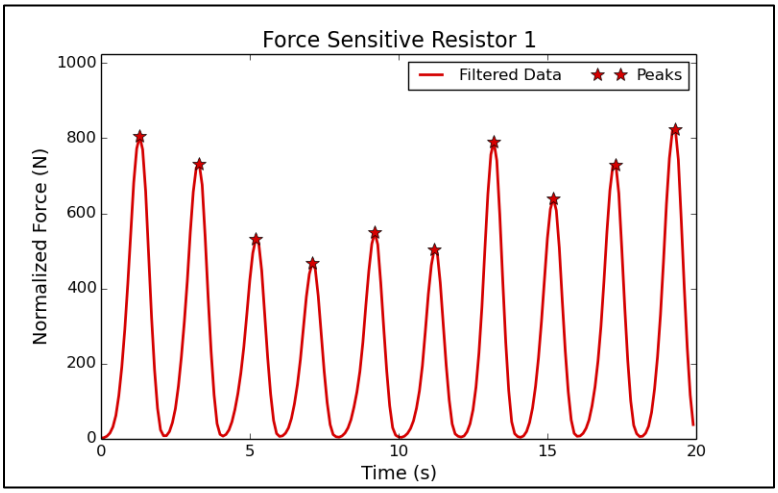

Figure 20: Filtered Data from FSR1

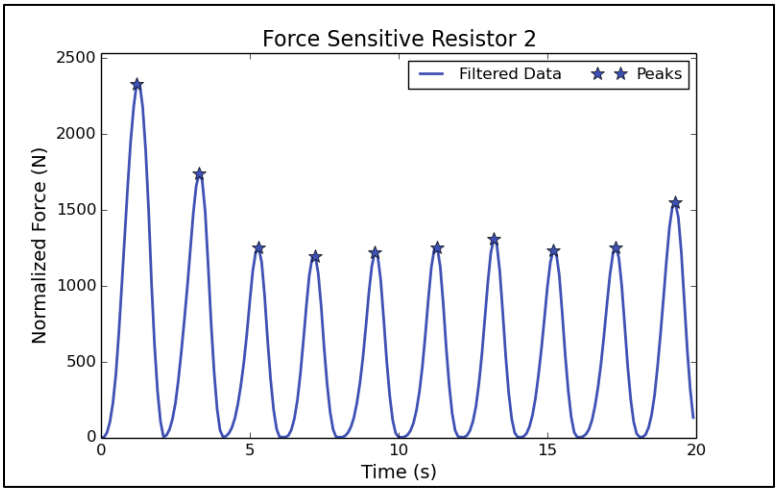

Figure 21: Filtered Data from FSR2

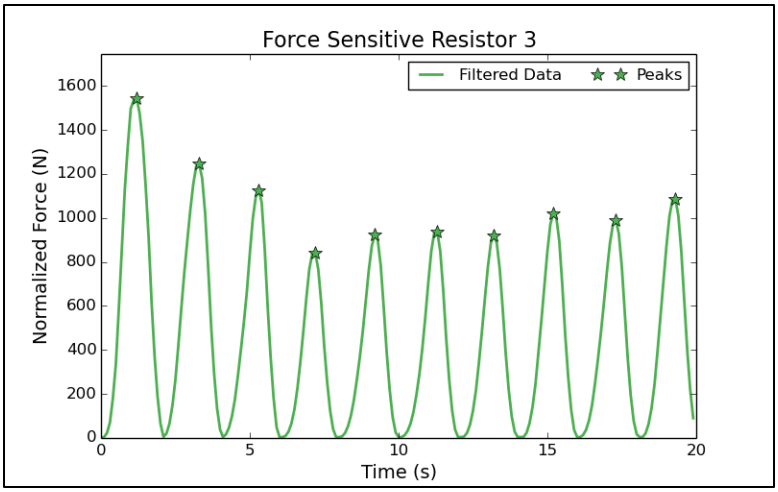

Figure 22: Filtered Data from FSR3

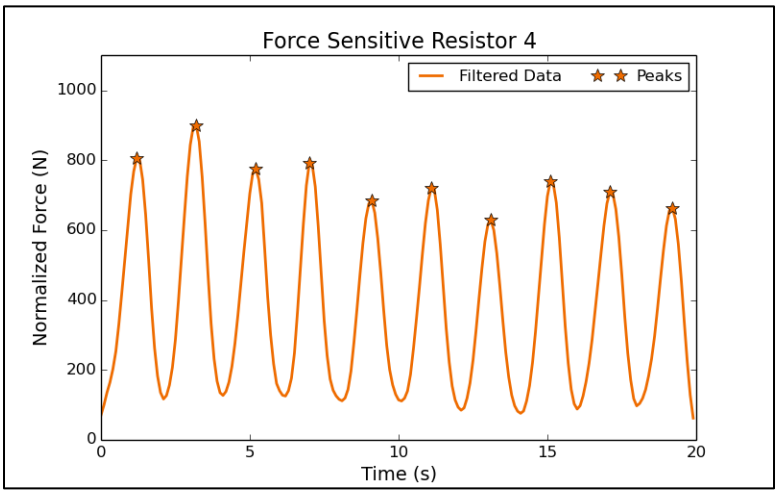

Figure 23: Filtered Data from FSR4

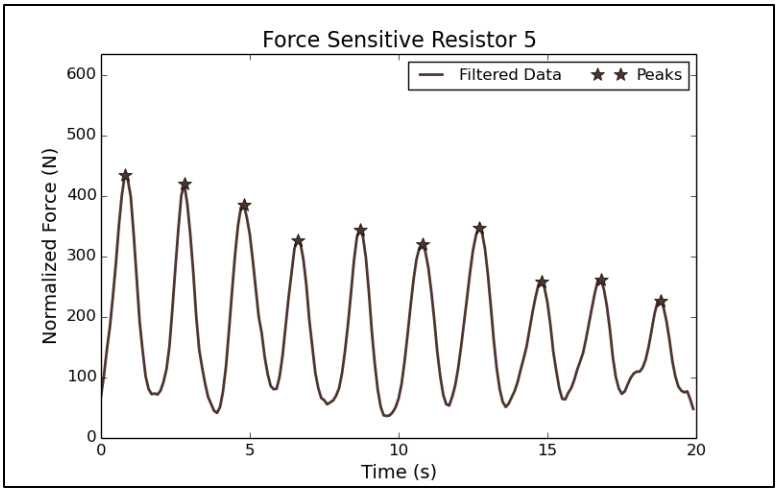

Figure 24: Filtered Data from FSR5

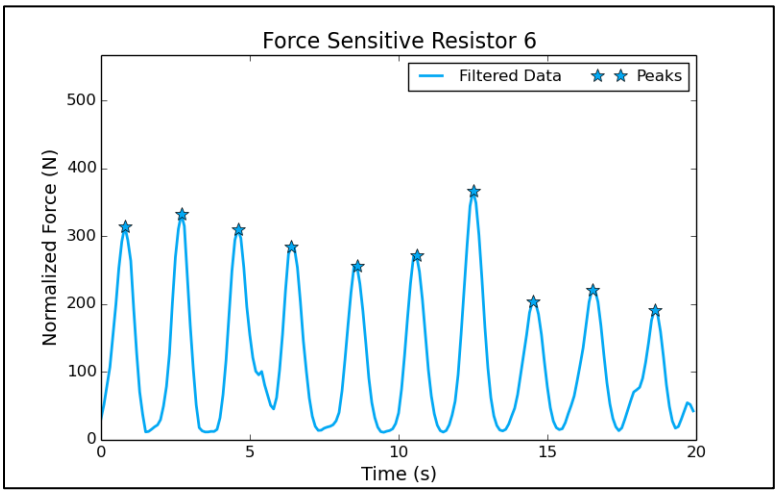

Figure 25: Filtered Data from FSR6

From Figure 26, with the help of complex algorithms, we can capture data related to the walking style or gait phase of the person. We can also monitor the changing pressure from different regions of the foot with respect to time. For instance, the first peaks are from FSR5 and FSR6, indicating that the bottom of the foot contacts the floor first. Later, we see peaks from FSR1 and FSR4, indicating that the mid foot strikes the floor. Lastly, we see peaks from FSR2 and FSR3, indicating that the hallux and toe region of the foot

contacting the floor. Thus, if sufficiently large amount of data is collected, we can establish a typical walking pattern among subjects of different age groups. Therefore, detecting abnormalities or biomedical ailments would be a mere comparison of statistical data and the data captured for a specific case.

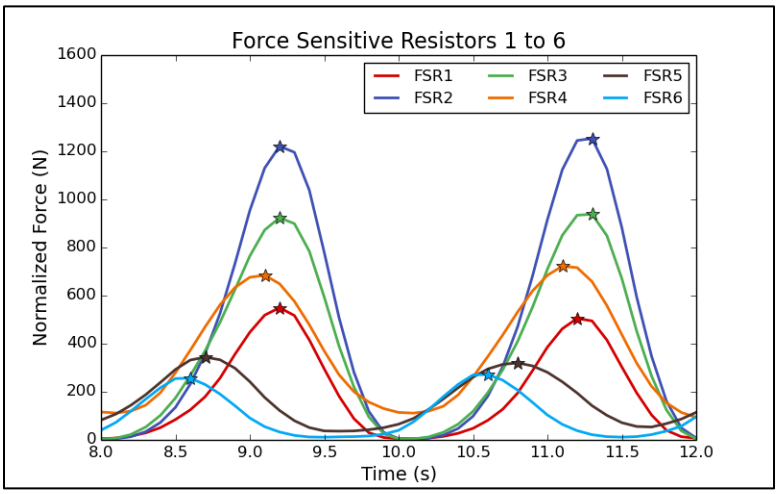

Figure 26: Filtered Data from All the FSR Sensors

Figure 27 through Figure 29 represent the data captured from the accelerometer within the motion sensor. Both original data and the filtered data are presented. Like the pressure sensor data, the motion data is filtered using a 5-point moving average filter to reduce high frequency noise. The data clearly shows regions of different activity. For instance, referring the time axis, from 0 to 5, we see that the variation in data is non-existent, which may indicate no activity. From 5 to 30, we have periodic variation indicating an activity such as walking or running, where each peak represents a swing of the foot. The data presented has approximately 20 peaks, indicating 20 swings of the right foot while walking 40 steps. To precisely classify the activity and to extract speed and direction information, further analysis is needed through techniques such as machine learning. The focus here is to

establish the fact that the data from motion sensor is extremely beneficial for determining and classifying different activities.

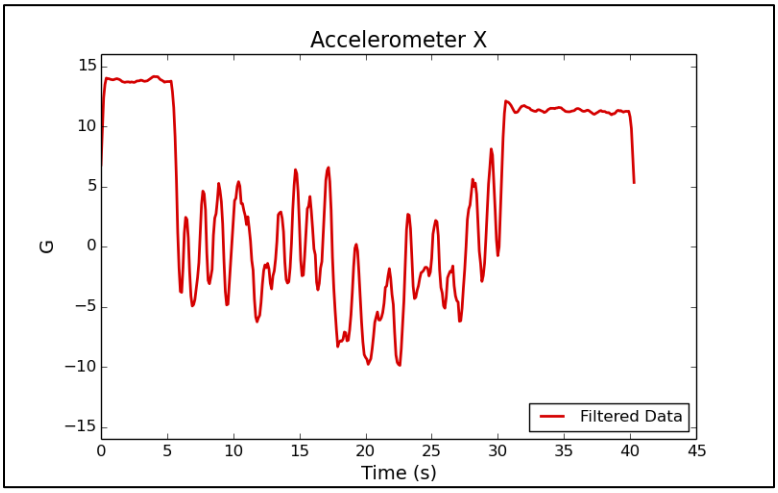

Figure 27: Filtered Data from the Accelerometer X Axis

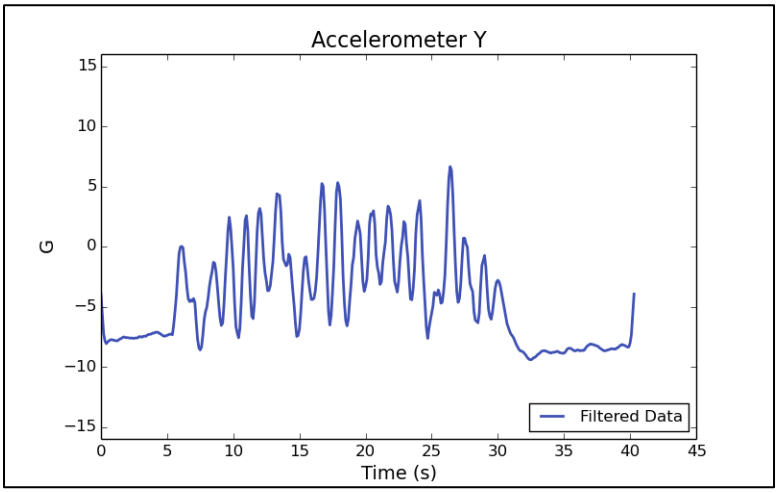

Figure 28: Filtered Data from the Accelerometer Y Axis

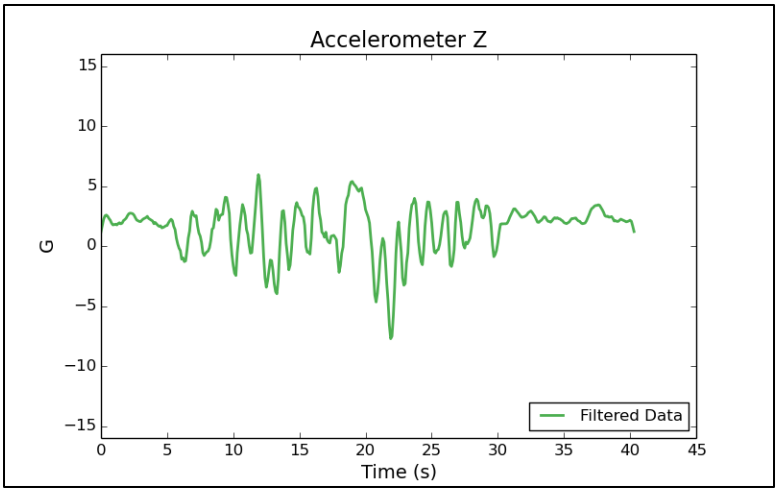

Figure 29: Filtered Data from the Accelerometer Z Axis

CHAPTER 6

6 CONCLUSION

In this work, the goal of developing a truly in-shoe force measurement system is accomplished. The device is designed in a way that it is suitable for everyday use. The comfort and the convenience of using the device in application areas such as biomedical, sports and fitness tracking was of importance. The goal of fitting the entire device within a shoe, without the need for any recording devices to be worn makes this a novel approach. The real-time data captured from the device can be accessed with the help of a BLE enabled smartphone. TI's starter app for iOS was used to receive the real-time BLE data from the device. Figure 30 represents a basic version of the app that presents real-time data from all the six pressure sensors, motion sensor and battery status information. This is the same data that was presented in the results section as original data from the pressure and motion sensor respectively.

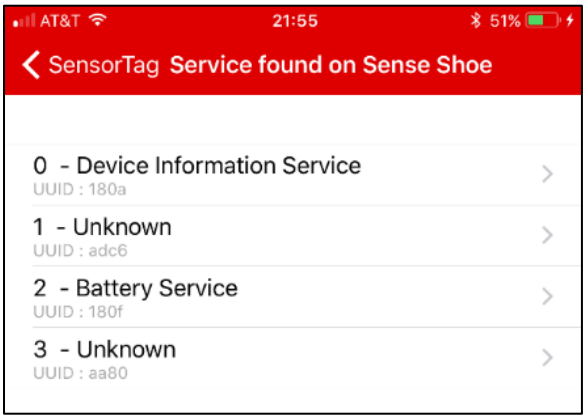

Figure 30: Smartphone App Interface

In the future work, the GUI for the app can be developed to display activity information presented in Table 6. In addition, the gait phase detection algorithm proposed by Hui et al. [1] could be easily incorporated to determine any abnormalities in the gait or walking style of the person. This could be beneficial in determining biomedical ailment. Moreover, with the incorporation of machine learning algorithms, the data from motion sensors can be processed and meaningful inferences such as speed, direction and angle of motion performed can be evaluated and presented for sports application.

REFERENCES

[1] Y. Hui, W. Dong-Hai, Y. Can-Jun, L. Kok-Meng, "A Walking Monitoring Shoe System for Simultaneous Plantar-force Measurement and Gait-phase Detection", IEEE/ASME International Conference on Advanced Intelligent Mechatronics, 2010.

[2] Kyoungchul Kong and M. Tomizuka, "A Gait Monitoring System Based on Air Pressure Sensors Embedded in a Shoe", IEEE/ASME Transactions on Mechatronics, vol. 14, no. 3, pp. 358-370, 2009.

[3] Lin Shu, Tao Hua, Yangyong Wang, Qiao Li, D. Feng and Xiaoming Tao, "In-Shoe Plantar Pressure Measurement and Analysis System Based on Fabric Pressure Sensing Array", IEEE Transactions on Information Technology in Biomedicine, vol. 14, no. 3, pp. 767-775, 2010.

[4] J. Stacy, L. Paul, D. Lee, M. Josh and R. Swarna, "Development of a Quantitative In-Shoe Measurement System for Assessing Balance: Sixteen-Sensor Insoles", IEEE EMBS, 2006.

[5] M. Saito, K. Nakajima, C. Takano, Y. Ohta, C. Sugimoto, R. Ezoe, K. Sasaki, H. Hosaka, T. Ifukube, S. Ino and K. Yamashita, "An in-shoe device to measure plantar pressure during daily human activity", Medical Engineering & Physics, vol. 33, no. 5, pp. 638-645, 2011.

[6] H. Hurkmans, J. Bussmann, E. Benda, J. Verhaar and H. Stam, "Techniques for measuring weight bearing during standing and walking", Clinical Biomechanics, vol. 18, no. 7, pp. 576-589, 2003.

[7] M. Hannula, A. Sakkinen and A. Kylmanen, "Development of EMFI-sensor based pressure sensitive insole for gait analysis", International Workshop on Medical Measurement and Applications, 2007.

[8] K. Antti, K. Jouni, P. Johan, T. Risto and H. Leila, "Wireless Weight Measurement Shoes", International Conference on Biomedical Engineering and Informatics, 2011.

[9] P. Matt and C. Brian, "Using a shoe mounted tri-axial accelerometer to detect kinematic changes during stiff ankle walking", IEEE EMBS, 2011.

[10] M. Hessert, M. Vyas, J. Leach, K. Hu, L. Lipsitz and V. Novak, "Foot pressure distribution during walking in young and old adults", BMC Geriatrics, vol. 5, no. 1, 2005.

[11] Abdul Razak, A. Zayegh, R. Begg and Y. Wahab, "Foot Plantar Pressure Measurement System: A Review", Sensors, vol. 12, no. 12, pp. 9884-9912, 2012.

[12] D. Low and S. Dixon, “Footscan pressure insoles: Accuracy and reliability of force and pressure measurements in running”, Gait & Posture, vol. 32, no. 4, pp. 664-666, 2010.

[13] H. Hurkmans, J. Bussmann, E. Benda, J. Verhaar and H. Stam, “Accuracy and repeatability of the Pedar Mobile system in long-term vertical force measurements”, Gait & Posture, vol. 23, no. 1, pp. 118-125, 2006.

[14] N. Carbonaro, F. Lorussi and A. Tognetti, “Assessment of a Smart Sensing Shoe for Gait Phase Detection in Level Walking”, Electronics, vol. 5, no. 4, p. 78, 2016.

[15] M. Chen, B. F. Huang, K. K. Lee and Y. S. Xu, “An Intelligent Shoe-Integrated System for Plantar Pressure Measurement”, IEEE International Conference on Robotics and Biomimetics, 2006.

[16] J. Park, Y. Na, G. Gu and J. Kim, “Flexible Insole Ground Reaction Force Measurement Shoes for Jumping and Running”, IEEE RAS & EMBS International Conference on Biomedical Robotics and Biomechatronics, 2016.

[17] T. Han, N. Paik and M. Im, “Quantification of the path of center of pressure (COP) using an F-scan in-shoe transducer”, Gait & Posture, vol. 10, no. 3, pp. 248-254, 1999.

[18] M. Brown, S. Rudicel and A. Esquenazi, “Measurement of Dynamic Pressures at the Shoe-Foot Interface During Normal Walking with Various Foot Orthoses Using the FSCAN System”, Foot & Ankle International, vol. 17, no. 3, pp. 152-156, 1996.

[19] J. Wertsch, J. Webster and W. Tompkins, “A portable insole plantar pressure measurement system”, The Journal of Rehabilitation Research and Development, vol. 29, no. 1, p. 13, 1992.

[20] L. Tracie and S. Robert, “Wireless in-shoe force system”, IEEE EMBS, vol. 5, pp. 2238-2241, 1997.

[21] M. Abhay and K. Nima, “The Applicability of an Athletic Shoe Comprising an In-Shoe Force Measurement System”, Barrett, The Honors College, Arizona State University, 2017.